References and Notes

1. Ishibashi M, Egashira K, Zhao Q, Hiasa K, Ohtani K, Ihara Y, Charo IF, Kura S, Tsuzuki T, Takeshita A, Sunagawa K. Bone marrow-derived monocyte chemoattractant protein-1 receptor ccr2 is critical in angiotensin ii-induced acceleration of atherosclerosis and aneurysm formation in hypercholesterolemic mice. *Arteriosclerosis, thrombosis, and vascular biology.* 2004;24:e174-178
2. Ni W, Kitamoto S, Ishibashi M, Usui M, Inoue S, Hiasa K, Zhao Q, Nishida K, Takeshita A, Egashira K. Monocyte chemoattractant protein-1 is an essential inflammatory mediator in angiotensin ii-induced progression of established atherosclerosis in hypercholesterolemic mice. *Arteriosclerosis, thrombosis, and vascular biology.* 2004;24:534-539
3. Egashira K. Molecular mechanisms mediating inflammation in vascular disease: Special reference to monocyte chemoattractant protein-1. *Hypertension.* 2003;41:834-841
4. Egashira K, Koyanagi M, Kitamoto S, Ni W, Kataoka C, Morishita R, Kaneda Y, Akiyama C, Nishida KI, Sueishi K, Takeshita A. Anti-monocyte chemoattractant protein-1 gene therapy inhibits vascular remodeling in rats: Blockade of mcp-1 activity after intramuscular transfer of a mutant gene inhibits vascular remodeling induced by chronic blockade of no synthesis. *FASEB J.* 2000;14:1974-1978
5. Egashira K, Nakano K, Ohtani K, Funakoshi K, Zhao G, Ihara Y, Koga J, Kimura S, Tominaga R, Sunagawa K. Local delivery of anti-monocyte chemoattractant protein-1 by gene-eluting stents attenuates in-stent stenosis in rabbits and monkeys. *Arteriosclerosis, thrombosis, and vascular biology.* 2007;27:2563-2568
6. Matoba T, Egashira K. Anti-inflammatory gene therapy for cardiovascular disease. *Curr Gene Ther.* 2011;11:442-446
7. Paigen B, Morrow A, Holmes PA, Mitchell D, Williams RA. Quantitative assessment of atherosclerotic lesions in mice. *Atherosclerosis.* 1987;68:231-240
8. Johnson J, Carson K, Williams H, Karanam S, Newby A, Angelini G, George S, Jackson C. Plaque rupture after short periods of fat feeding in the apolipoprotein e-knockout mouse: Model characterization and effects of pravastatin treatment. *Circulation.* 2005;111:1422-1430
9. Tacke F, Alvarez D, Kaplan TJ, Jakubzick C, Spanbroek R, Llodra J, Garin A, Liu J, Mack M, van Rooijen N, Lira SA, Habenicht AJ, Randolph GJ. Monocyte subsets differentially employ ccr2, ccr5, and cx3cr1 to accumulate within atherosclerotic plaques. *The Journal of clinical investigation.* 2007;117:185-194
10. Swirski FK, Nahrendorf M, Etzrodt M, Wildgruber M, Cortez-Retamozo V, Panizzi P, Figueiredo JL, Kohler RH, Chudnovskiy A, Waterman P, Aikawa E, Mempel TR, Libby P, Weissleder R, Pittet MJ. Identification of splenic reservoir monocytes and their

deployment to inflammatory sites. *Science.* 2009;325:612-616

11. Kubo M, Egashira K, Inoue T, Koga J, Oda S, Chen L, Nakano K, Matoba T, Kawashima Y, Hara K, Tsujimoto H, Sueishi K, Tominaga R, Sunagawa K. Therapeutic neovascularization by nanotechnology-mediated cell-selective delivery of pitavastatin into the vascular endothelium. *Arteriosclerosis, thrombosis, and vascular biology.* 2009;29:796-801
12. Oda S, Nagahama R, Nakano K, Matoba T, Kubo M, Sunagawa K, Tominaga R, Egashira K. Nanoparticle-mediated endothelial cell-selective delivery of pitavastatin induces functional collateral arteries (therapeutic arteriogenesis) in a rabbit model of chronic hind limb ischemia. *J Vasc Surg.* 2010;52:412-420
13. Chen L, Nakano K, Kimura S, Matoba T, Iwata E, Miyagawa M, Tsujimoto H, Nagaoka K, Kishimoto J, Sunagawa K, Egashira K. Nanoparticle-mediated delivery of pitavastatin into lungs ameliorates the development and induces regression of monocrotaline-induced pulmonary artery hypertension. *Hypertension.* 2011;57:343-350
14. Satoh K, Nigro P, Matoba T, O'Dell MR, Cui Z, Shi X, Mohan A, Yan C, Abe J, Illig KA, Berk BC. Cyclophilin a enhances vascular oxidative stress and the development of angiotensin ii-induced aortic aneurysms. *Nat Med.* 2009;15:649-656
15. Ishibashi M, Hiasa K, Zhao Q, Inoue S, Ohtani K, Kitamoto S, Tsuchihashi M, Sugaya T, Charo IF, Kura S, Tsuzuki T, Ishibashi T, Takeshita A, Egashira K. Critical role of monocyte chemoattractant protein-1 receptor ccr2 on monocytes in hypertension-induced vascular inflammation and remodeling. *Circ Res.* 2004;94:1203-1210
16. Han KH, Ryu J, Hong KH, Ko J, Pak YK, Kim JB, Park SW, Kim JJ. Hmg-coa reductase inhibition reduces monocyte cc chemokine receptor 2 expression and monocyte chemoattractant protein-1-mediated monocyte recruitment in vivo. *Circulation.* 2005;111:1439-1447

Supplementary Figure Legends

Supplementary Figure 1. Experimental protocols for the treatments in $ApoE^{-/-}$ mice. At 16-18 weeks of age, mice began receiving the HFD. After 4 weeks of the experimental diet, all mice were infused with angiotensin II dissolved in phosphate-buffered saline (PBS) at 1.9 mg/kg per day.

Protocol 1. Animals were divided into 2 groups at the beginning of angiotensin II infusion: (i) adoptively transferred $CCR2^{+/+}$-inflammatory macrophages from $ApoE^{-/-}$ mice (1×10^6 cells/ 200 μl PBS) and (ii) adoptively transferred $CCR2^{-/-}$-leukocytes from $ApoE^{-/-}CCR2^{-/-}$ mice (1×10^6 cells/ 200 μl PBS).

Protocol 2. Animals were divided into 2 groups at the beginning of angiotensin II infusion: (i) the FITC-incorporated NP group (1.3 mg PLGA/ 200 μl PBS) and (ii) the 7ND-incorporated NP group (5 μg 7ND plasmid/ 200 μl PBS). NPs were administered by weekly intravenous injection.

Protocol 3. Animals were divided into 4 groups at the beginning of angiotensin II infusion: (i) the no treatment group, (ii) the FITC-incorporated NP group (0.1 mg PLGA/ 200 μl PBS), (iii) the pitavastatin-only group (0.012 mg pitavastatin/ 200 μl PBS), and (iv) the pitavastatin-incorporated NP group (0.1 mg PLGA/ 0.012 mg pitavastatin/ 200 μl PBS). NPs were administered by weekly intravenous injection.

Protocol 4. Animals were divided into 2 groups at the beginning of angiotensin II infusion: (i) oral daily administration of pitavastatin at a low dose (0.1 mg/kg/day) and (ii) oral daily administration of pitavastatin at a high dose (1.0 mg/kg/day). Pitavastatin was daily administered by oral gavage.

The no treatment group in protocol 2 was also used as the control group in protocols 1. and 4.

Supplementary Figure 2. Characteristics and kinetics of adoptive transferred macrophages. (**A**) Quantitative flow cytometric analysis of the number of $F4/80^+CD115^+$ macrophages in the peritoneal cavities of $ApoE^{-/-}$ or $ApoE^{-/-}CCR2^{-/-}$ mice induced by intraperitoneal injection of thioglycollate (TG). (**B**) Quantitative analysis of the mean

fluorescence intensity (MFI) of Ly-6C expression in the $F4/80^{+}CD115^{+}$ macrophages from the peritoneal cavities of the $ApoE^{-/-}$ mice. The data are reported as the mean±SEM. (**C**) Left panel: A fluorescence photomicrograph of the brachiocephalic artery of an $ApoE^{-/-}$ mouse from the no treatment group. Upper middle and right panel: PKH fluorescence photomicrographs of the brachiocephalic artery of an $ApoE^{-/-}$ mouse transferred with PKH-labeled activated macrophages. Lower middle and right panel: FITC autofluorescence photomicrographs of the brachiocephalic artery of an $ApoE^{-/-}$ mouse transferred with PKH-labeled activated macrophages. Right panel: An expanded image of the red square area in the middle panel. The nuclei were stained with DAPI. The scale bar indicates 100 μm.

Supplementary Figure 3. The adoptive transfer of splenic monocytes accelerates plaque destabilization and rupture in the brachiocephalic arteries. (A) Left panel: Representative flow cytometry dot plots of splenic leukocytes from $ApoE^{-/-}$ mice. Middle panel: The Representative flow cytometry dot plots of splenic leukocytes negatively selected with antibodies against the leukocytes other than monocytes from $ApoE^{-/-}$ mice. Right panel: The Representative histogram of Ly-6C expression on negatively selected splenic monocytes. (B) Upper panel: Photomicrographs of atherosclerotic plaques in the brachiocephalic artery stained with elastica van Gieson (EVG) in the No Treatment (N) and the Monocytes (M) groups. Arrowheads indicate disrupted/buried fibrous caps. The scale bar indicates 100 μm. Lower panel: Quantitation of the number of disrupted/buried fibrous caps and fibrous cap thickness. The data are reported as the mean±SEM. $*P<0.05$ versus the No Treatment group. There were no statistically significant differences in fibrous cap thickness between the two groups.

Supplementary Figure 4. Cellular uptake and *in vitro* kinetics of the NPs in macrophages. (**A**) Fluorescence photomicrographs of murine peritoneal macrophages incubated with FITC-NPs for 24 hours. An inset depicts a photomicrograph of macrophages incubated without FITC-NPs. (**B**) A fluorescence confocal microscopy image of RAW264.7 cells

incubated with FITC-NPs for 24 hours. (**C**) Electron microscopy image of RAW264.7 cells incubated with OsO_4-NPs for 24 hours. (**D**) Upper panel: Time course of the FITC signal retained in RAW264.7 cells after a 2-hour incubation with FITC-NPs or FITC (0.3, 1, 3, 10, 30, 100 μM) followed by a washout period. Cells were observed at 0, 24, 72 hours, and 1 week of washout. Lower panel: Quantitative analysis of relative fluorescence units (RFUs) of RAW264.7 cells incubated with FITC-NPs (green lines) or FITC (blue lines). $*P<0.01$ and $**P<0.001$ versus FITC (N = 4 per group). Data were compared using two-way ANOVA followed by Bonferroni's multiple comparison tests.

Supplementary Figure 5. Effects of daily oral administration of pitavastatin (0.1 or 1.0 mg/kg per day) on atherosclerotic plaque rupture in the brachiocephalic arteries. (**A**) Upper panel: Photomicrographs of atherosclerotic plaques stained with elastica van Gieson (EVG), Mac3 or MCP-1 in the No Treatment (N), pitavastatin 0.1 mg/kg (0.1), and pitavastatin 1.0 mg/kg (1.0) groups. Arrowheads indicate disrupted/buried fibrous caps. The scale bar indicates 100 μm. Lower panel: Quantitation of the number of disrupted/buried fibrous caps, fibrous cap thickness and Mac3- and MCP-1-positive areas. The data are reported as the mean±SEM. $\dagger P<0.05$ versus the No Treatment group using one-way ANOVA followed by Dunnett's multiple comparison tests. $**P<0.01$ versus the No Treatment group using one-way ANOVA followed by Bonferroni's multiple comparison tests. (**B**) Upper panel: Photomicrographs of the intraluminal surface of the total aorta stained with oil red O. Lower panel: Quantitation of the percentage of the plaque area compared with the total luminal surface area. The data are reported as the mean±SEM. $*P<0.05$ versus the No Treatment group. (C) Upper panel: Photomicrographs of atherosclerotic plaques in the aortic root stained with EVG or Mac3. Lower panel: Quantitation of plaque size and Mac3-positive areas. The scale bar indicates 200 μm. The data are reported as the mean±SEM. $\dagger P<0.05$ versus the No Treatment group using one-way ANOVA followed by Dunnett's multiple comparison tests.

Supplementary Tables

Supplementary Table 1. Body weight, heart rate, systolic blood pressure, and lipid profiles in the no treatment, $CCR2^{+/+}$ inflammatory macrophage, and $CCR2^{-/-}$ leukocyte groups.

	No Treatment (N= 9)	$CCR2^{+/+}$ Inflammatory Macrophage (N= 5)	$CCR2^{-/-}$ Leukocyte (N= 8)
Body Weight (g)	33±1	35±3	34±3
Heart Rate (beat/min)	650±20	640±40	580±40
Systolic Blood Pressure (mmHg)	120±2	112±8	115±9
Total Cholesterol (mg/dl)	660±30	710±100	720±60
Triglyceride (mg/dl)	65±9	74±16	69±5

The data are expressed as the mean±SEM. The mean values were compared using ANOVA and Bonferroni's multiple comparison tests, and there are no significant differences for any of these parameters among these groups.

Supplementary Table 2. Body weight, heart rate, systolic blood pressure, and lipid profiles in the no treatment, FITC-NP, pitavastatin, and pitavastatin-NP groups.

	No Treatment (N= 9)	FITC-NP (N= 7)	Pitava (N= 6)	Pitava-NP (N= 10)
Body Weight (g)	33±1	30±1	34±1	32±1

Heart Rate (beat/min)	650±20	630±30	650±20	590±20
Systolic Blood Pressure (mmHg)	120±0	110±10	12±10	120±0
Total Cholesterol (mg/dl)	660±30	670±50	610±50	710±40
Triglyceride (mg/dl)	65±9	60±5	53±5	70±6

The data are expressed as the mean±SEM. The mean values were compared using ANOVA and Bonferroni's multiple comparison tests, and there are no significant differences for any of these parameters compared with the No Treatment group.

Supplementary Table 3. Body weight, heart rate, systolic blood pressure, and lipid profiles in the FITC-NP and 7ND-NP groups.

	FITC-NP (N= 9)	7ND-NP (N= 10)
Body Weight (g)	28±1	25±1
Heart Rate (beat/min)	640±30	680±10
Systolic Blood Pressure (mmHg)	130±10	120±10
Total Cholesterol (mg/dl)	720±60	730±20
Triglyceride (mg/dl)	47±11	53±18

The data are expressed as the mean±SEM. The mean values were compared using the unpaired *t*-test, and there are no significant differences for any of these parameters between these 2 groups.

Supplementary Table 4. Body weight, heart rate, systolic blood pressure, and lipid profiles in the no treatment, pitavastatin 0.1 mg/kg, and pitavastatin 1.0 mg/kg groups.

	No Treatment (N= 9)	Pitavastatin 0.1 mg/kg (N= 10)	Pitavastatin 1.0 mg/kg (N= 11)
Body Weight (g)	33±1	30±1*	32±0
Heart Rate (beat/min)	650±20	610±20	630±10
Systolic Blood Pressure (mmHg)	120±0	110±0	120±0
Total Cholesterol (mg/dl)	660±30	780±20	800±50
Triglyceride (mg/dl)	65±9	82±15	43±5

The data are expressed as the mean±SEM. *P<0.05 versus the No Treatment group. The data were compared using ANOVA followed by Bonferroni's multiple comparison tests.

Supplementary Table 5. Serum biomarkers in the no treatment, $CCR2^{+/+}$ inflammatory macrophage, and $CCR2^{-/-}$ leukocyte group.

		No Treatment (N= 7)	$CCR2^{+/+}$ Inflammatory Macrophage (N= 5)	$CCR2^{-/-}$ Leukocyte (N= 7)
Apo A1	**μg/mL**	48±6	39±6	38±3
CD40	**pg/mL**	87±9	160±40	75±9
CD40 Ligand	**pg/mL**	2600±300	5700±400**	4600±700*
CRP	**μg/mL**	11±1	10±1	11±2

EGF	**pg/mL**	16±1	23±1**	21±1**
Endothelin-1	**pg/mL**	18±1	21±2	17±2
Eotaxin	**pg/mL**	320±20	330±50	380±30
Factor VII	**ng/mL**	14±1	19±1*	18±1
FGF-basic	**ng/mL**	7.0±0.6	11±1*	9.0±0.8
GCP-2	**ng/mL**	31±7	13±7	5±1**
Haptoglobin	**μg/mL**	140±20	190±30	200±20
IFN-γ	**pg/mL**	N.D.	23±8	N.D.
IgA	**μg/mL**	42±5	52±9	60±7
IL-10	**pg/mL**	430±20	N.D.	N.D.
IL-11	**pg/mL**	N.D.	490±430	85±29
IL-17	**ng/mL**	N.D.	N.D.	0.01±0.00
IL-18	**ng/mL**	18±1	30±1***	27±0***
IL-1α	**pg/mL**	260±72	160±45	94±15
IL-1β	**ng/mL**	17±1	20±1	20±1
IL-5	**ng/mL**	N.D.	0.73±0.23	0.61±0.12
IL-6	**pg/mL**	11±2	15±4	N.D.
IL-7	**ng/mL**	0.18±0.06	0.22±0.12	0.18±0.07
IP-10	**pg/mL**	68±9	230±140	54±3
LIF	**pg/mL**	1200±0	1500±100	1200±100
Lymphotactin	**pg/mL**	120±50	180±40	100±20
MCP-1	**pg/mL**	130±10	220±30**	110±10
MCP-3	**pg/mL**	400±30	700±100**	490±40
MCP-5	**pg/mL**	21±2	49±6**	37±6

M-CSF	**ng/mL**	5.2±0.3	8.2±0.4***	6.0±0.1
MDC	**pg/mL**	460±20	580±70	560±40
MIP-1α	**ng/mL**	2.4±0.3	4.1±0.2***	4.0±0.2***
MIP-1β	**pg/mL**	190±40	410±50**	280±20
MIP-1γ	**ng/mL**	50±3	67±7	52±7
MIP-2	**pg/mL**	18±4	28±3	21±2
MIP-3	**ng/mL**	2.3±0.2	3.5±0.3**	2.4±0.3
MMP-9	**ng/mL**	110±20	210±20**	140±20
MPO	**ng/mL**	110±20	200±10**	160±10*
Myoglobin	**ng/mL**	320±260	260±200	78±32
OSM	**ng/mL**	0.15±0.03	N.D.	0.03±0.01**
RANTES	**pg/mL**	0.64±0.20	N.D.	N.D.
SAP	**μg/mL**	47±2	35±1*	38±4
SCF	**pg/mL**	310±40	230±30	190±20*
SGOT	**μg/mL**	51±9	50±5	73±4
TIMP-1	**ng/mL**	4.9±0.7	5.2±0.9	4.7±0.6
Tissue Factor	**ng/mL**	8.6±0.3	11±2	7.5±1.0
TNF-α	**ng/mL**	0.11±0.02	N.D.	N.D.
TPO	**ng/mL**	110±10	150±10**	130±0*
VCAM-1	**ng/mL**	2200±100	3500±700*	2700±100
VEGF	**pg/mL**	290±40	200±10	190±10*
vWF	**ng/mL**	150±10	330±130	160±20

The data are expressed as the mean±SEM. The means were compared by means of

ANOVA and Bonferroni's multiple comparison tests. **P*<0.05 versus the No Treatment group, ***P*<0.01 versus the No Treatment group, ****P*<0.001 versus the No Treatment group. Multiplex immunoassay was performed using the Luminex LabMAP instruments by Charles River Inc. Apo A1 (Apolipoprotein A1), CD (Cluster of Differentiation), CRP (C Reactive Protein), EGF (Epidermal Growth Factor), FGF-9 (Fibroblast Growth Factor-9), FGF-basic (Fibroblast Growth Factor-basic), GCP-2 (Granulocyte Chemotactic Protein-2), GM-CSF (Granulocyte Macrophage-Colony Stimulating Factor), GST-α (Glutathione S-Transferase alpha), IFN-γ (Interferon-gamma), IgA (Immunoglobulin A), IL (Interleukin), IP-10 (Inducible Protein-10), KC/GROα (Melanoma Growth Stimulatory Activity Protein), LIF (Leukemia Inhibitory Factor), MCP (Monocyte Chemoattractant Protein), M-CSF (Macrophage Colony-Stimulating Factor), MDC (Macrophage-Derived Chemokine), MIP (Macrophage Inflammatory Protein), MMP-9 (Matrix Metalloproteinase-9), MPO (Myeloperoxidase), OSM (Oncostatin M), RANTES (Regulation Upon Activation, Normal T-Cell Expressed and Secreted), SAP (Serum Amyloid P), SCF (Stem Cell Factor), SGOT (Serum Glutamic-Oxaloacetic Transaminase), TIMP-1 (Tissue Inhibitor of Metalloproteinase Type-1), TNF-α (Tumor Necrosis Factor-alpha), TPO (Thrombopoietin), VCAM-1 (Vascular Cell Adhesion Molecule-1), VEGF (Vascular Endothelial Cell Growth Factor), vWF (von Willebrand Factor). N.D. (Not Detected).

Supplementary Table 6. Serum biomarkers in the FITC-NP and pitavastatin-NP groups.

		FITC-NP (N= 6)	Pitava-NP (N= 9)
Apo A1	**μg/mL**	45±2	46±2

CD40	**pg/mL**	110±10	90±11
CD40 Ligand	**pg/mL**	1900±100	1400±100*
CRP	**μg/mL**	7.6±0.8	7.5±0.8
EGF	**pg/mL**	26±3	24±1
Endothelin-1	**pg/mL**	24±2	24±1
Eotaxin	**pg/mL**	370±10	420±20
Factor VII	**ng/mL**	28±2	28±1
FGF-basic	**ng/mL**	17±2	17±0
GCP-2	**ng/mL**	39±5	35±4
Haptoglobin	**μg/mL**	150±10	150±10
IgA	**μg/mL**	44±12	32±3
IL-10	**pg/mL**	N.D.	N.D.
IL-11	**pg/mL**	120±60	61±9
IL-18	**ng/mL**	18±1	16±1
IL-1α	**pg/mL**	440±130	200±40
IL-1β	**ng/mL**	7.9±0.3	7.8±0.6
IL-4	**pg/mL**	71±28	59±6
IL-5	**ng/mL**	0.80±0.12	1.1±0.2
IL-6	**pg/mL**	N.D.	12±4
IL-7	**ng/mL**	0.082±0.018	N.D.
IP-10	**pg/mL**	40±3	47±7
LIF	**pg/mL**	1900±100	1900±100
Lymphotactin	**pg/mL**	80±9	82±7
MCP-1	**pg/mL**	130±10	110±0*

MCP-3	**pg/mL**	380±30	320±20
MCP-5	**pg/mL**	28±4	30±2
M-CSF	**ng/mL**	7.3±0.1	7.5±0.2
MDC	**pg/mL**	650±40	840±70
MIP-1α	**ng/mL**	3.3±0.2	3.2±0.1
MIP-1β	**pg/mL**	200±30	180±10
MIP-1γ	**ng/mL**	54±4	45±3
MIP-2	**pg/mL**	28±2	22±2
MIP-3	**ng/mL**	2.0±0.1	2.1±0.1
MMP-9	**ng/mL**	130±10	120±10
MPO	**ng/mL**	140±20	120±10
Myoglobin	**ng/mL**	240±60	360±150
OSM	**ng/mL**	0.05±0.01	N.D.
SAP	**μg/mL**	32±2	30±2
SCF	**pg/mL**	280±10	240±10*
TIMP-1	**ng/mL**	5.0±0.7	4.3±0.5
Tissue Factor	**ng/mL**	14±1	12±0
TPO	**ng/mL**	30±3	32±2
VCAM-1	**ng/mL**	2600±100	2500±200
VEGF	**pg/mL**	200±20	150±10*
vWF	**ng/mL**	180±10	150±10*

The data are expressed as the mean±SEM. The mean values were compared using an unpaired *t*-test. *$P<0.05$ versus the FITC-NP group.

Supplementary Table 7. Plasma concentration of pitavastatin in the pitavastatin and pitavastatin-NP groups.

	2 hours	6 hours	24 hours
Pitavastatin (ng/mL)	1.3±0.2	N.D.	N.D.
Pitavastatin-NP (ng/mL)	2.5±0.2*	N.D.	N.D.

The data are expressed as the mean±SEM. The mean values were compared using an unpaired *t*-test. *$P<0.05$ versus the Pitavastatin group.

Experiment Protocol 1

ApoE$^{-/-}$mice or ApoE$^{-/-}$CCR2$^{-/-}$mice
Thioglycollate-induced
peritoneal macrophages

↓

ApoE$^{-/-}$mice
18 weeks of age

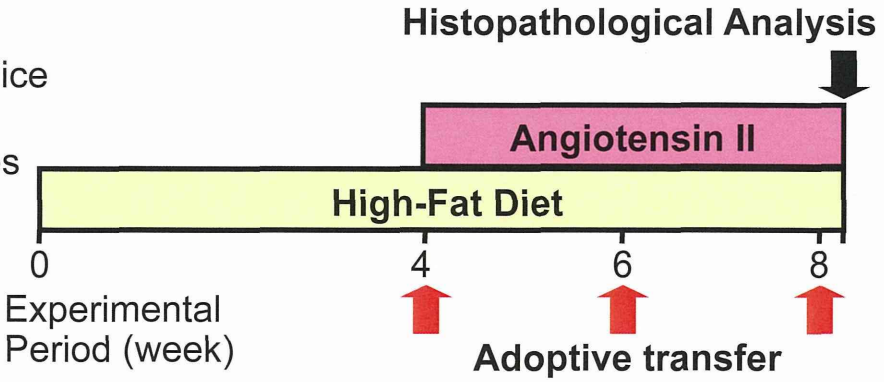

Treatment Group

1. CCR2$^{+/+}$-Inflammatory Macrophage (1x10^6 cells/ 200 μL PBS)
2. CCR2$^{-/-}$-Leukocyte (1x10^6 cells/ 200 μL PBS)

Experiment Protocol 2

ApoE$^{-/-}$mice
16 weeks of age

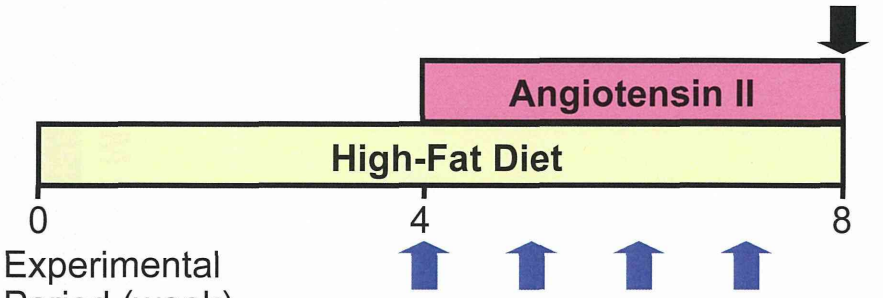

Treatment Group

1. No treatment
2. FITC-NP (0.1 mg PLGA/ 200 μL PBS)
3. Pitavastatin (Pitavastatin 0.012 mg/ 200 μL PBS)
4. Pitavastatin-NP (0.1 mg PLGA/ Pitavastatin 0.012 mg/ 200 μL PBS)

Experiment Protocol 3

ApoE$^{-/-}$mice
16 weeks of age

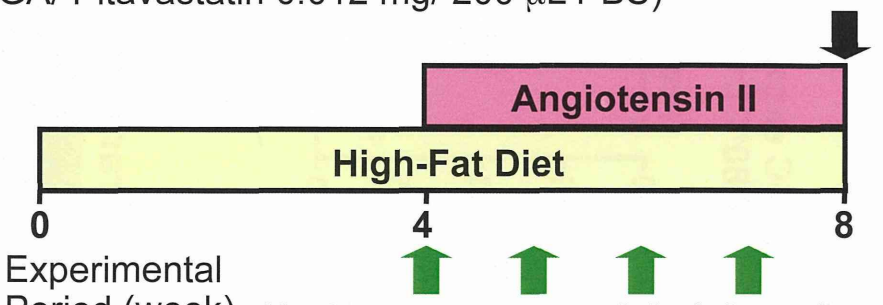

Treatment Group

1. FITC-NP (1.3 mg PLGA/ 200 μL PBS)
2. 7ND-NP (1.3 mg PLGA/ 5 μg 7ND plasmid/ 200 μL PBS)

Experiment Protocol 4

ApoE$^{-/-}$mice
16 weeks of age

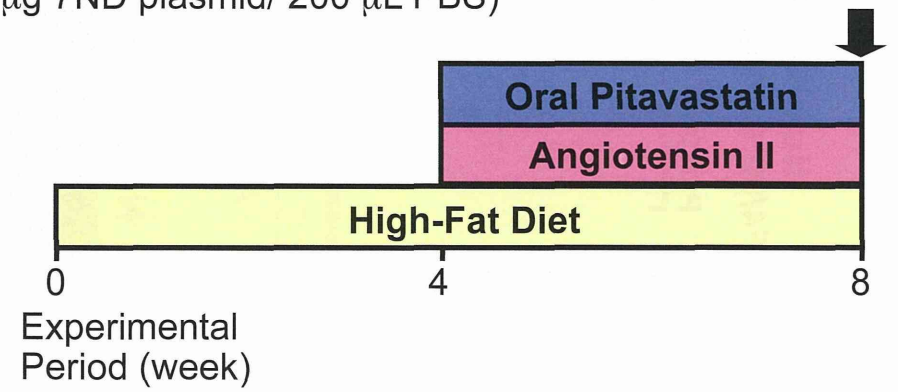

Treatment Group

1. Pitavastatin (Lower dose: 0.1 mg/kg/day)
2. Pitavastatin (Higher dose: 1.0 mg/kg/day)

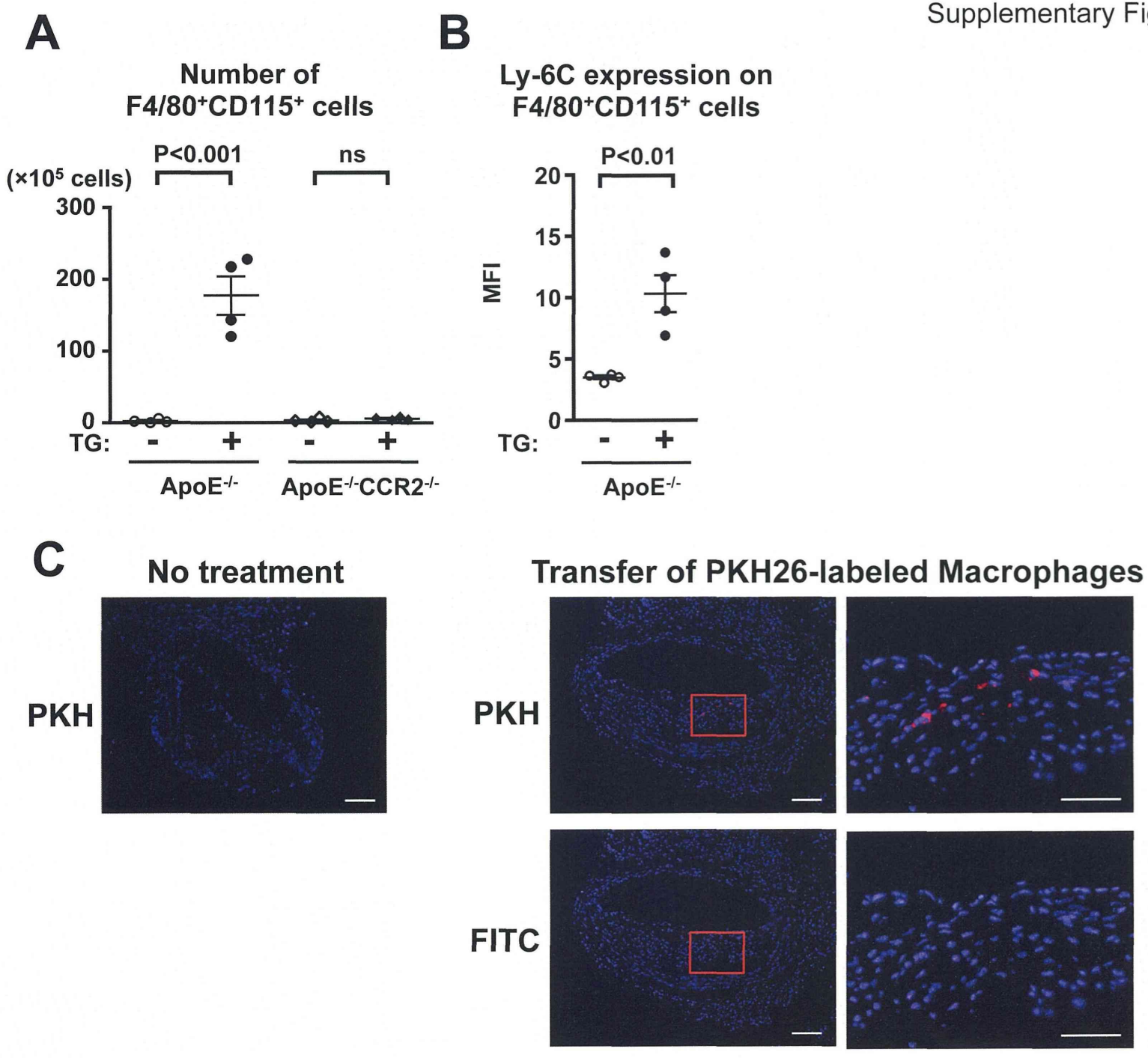
A
Number of
F4/80+CD115+ cells
P<0.001
ns
(×10⁵ cells)
300
200
100
0
TG: - + - +
ApoE-/-
ApoE-/-CCR2-/-
B
Ly-6C expression on
F4/80+CD115+ cells
P<0.01
MFI
20
15
10
5
0
TG: - +
ApoE-/-
C
No treatment
Transfer of PKH26-labeled Macrophages
PKH
PKH
FITC

Supplementary Figure 3, Katsuki S et al

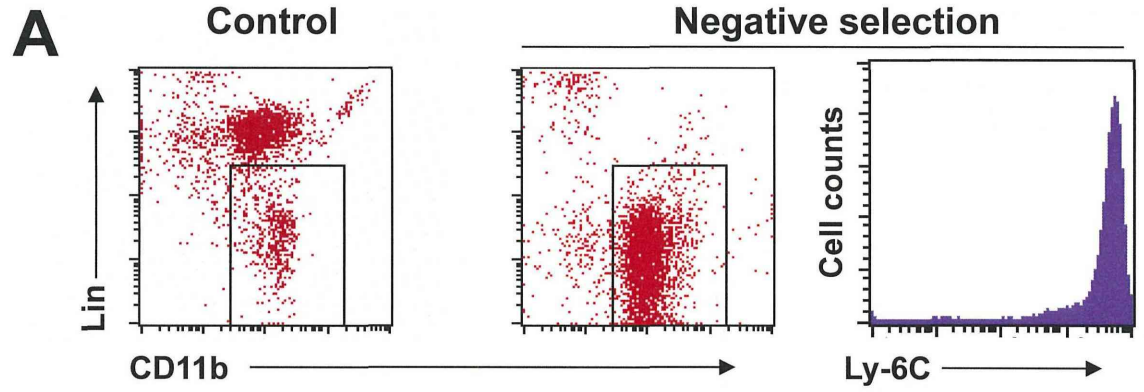

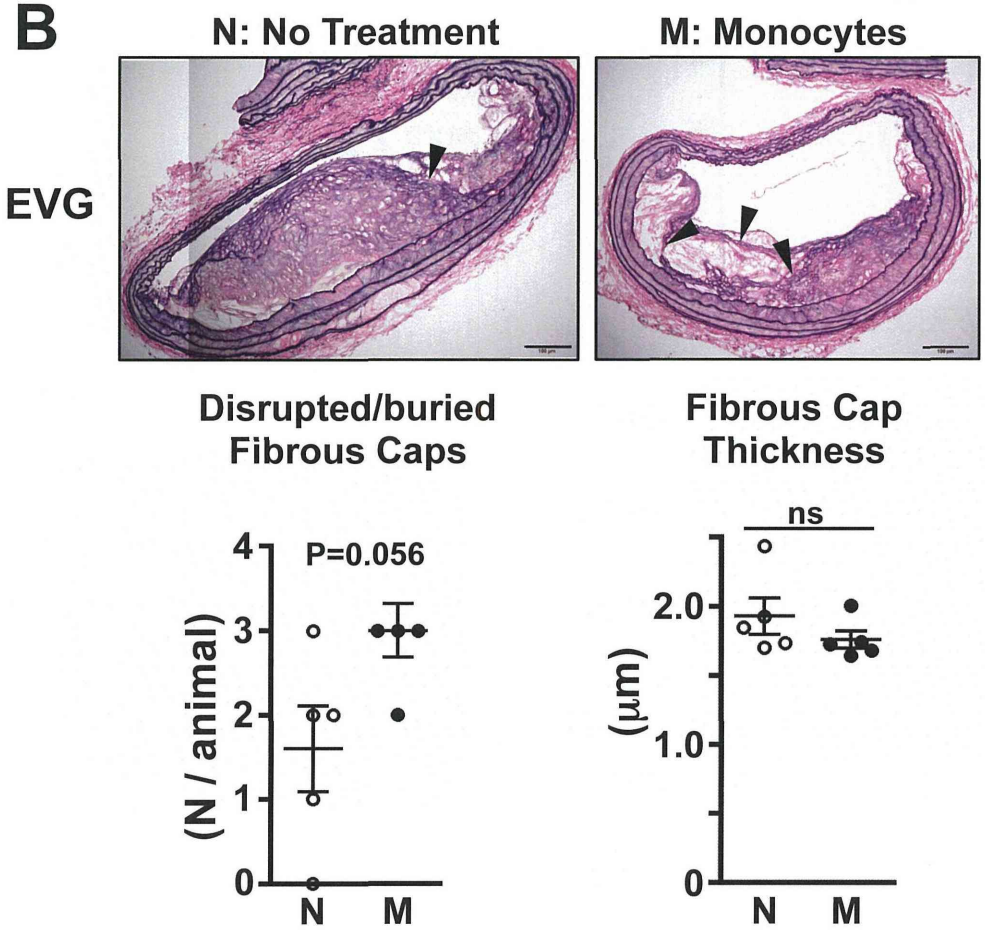

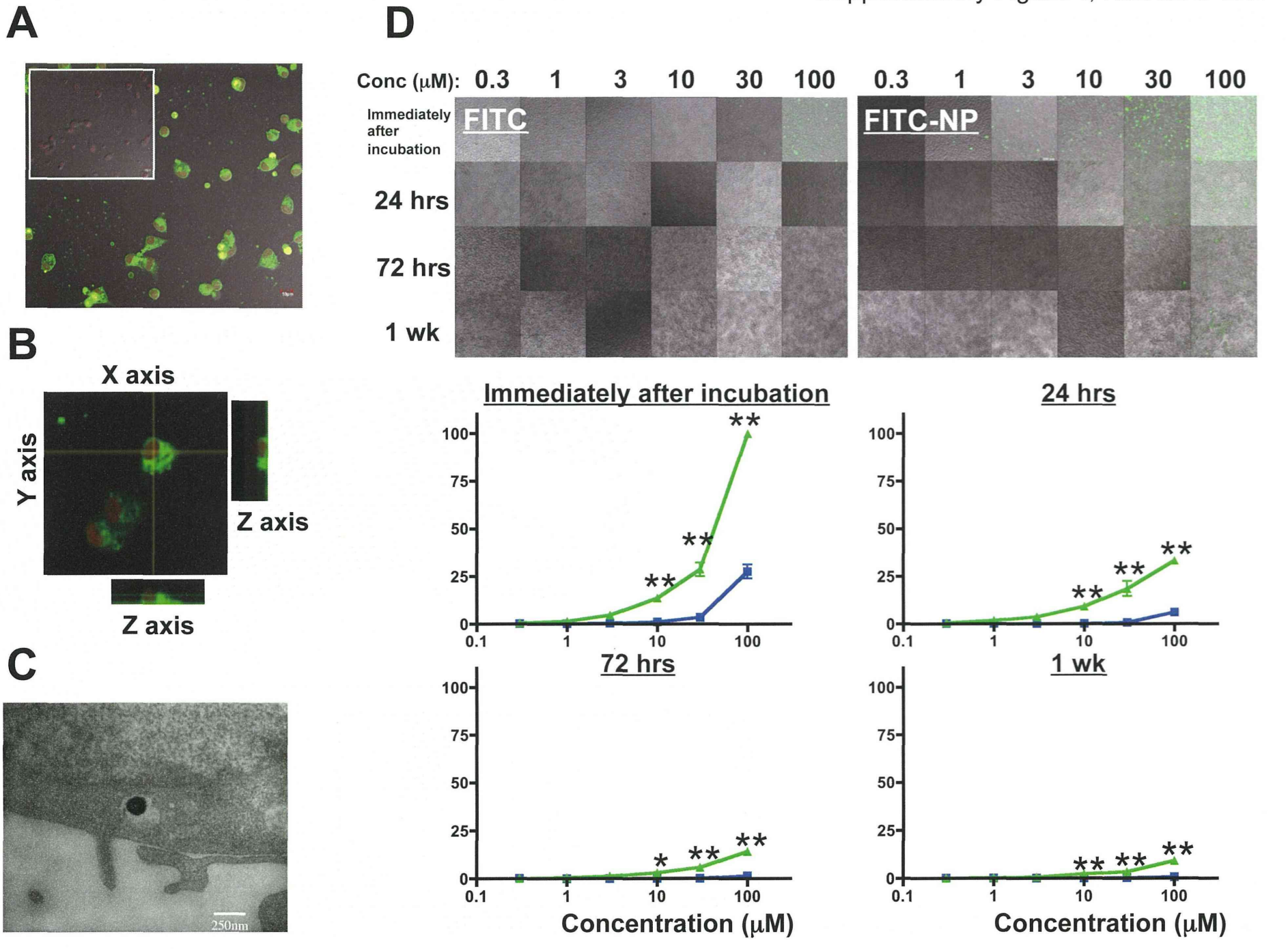
A
B
X axis
Y axis
Z axis
Z axis
C
250nm
D
Conc (μM): 0.3 1 3 10 30 100 0.3 1 3 10 30 100
Immediately after incubation
24 hrs
72 hrs
1 wk
FITC
FITC-NP
Immediately after incubation
24 hrs
72 hrs
1 wk
100
75
50
25
0
0.1
1
10
100
**
*
Concentration (μM)

Supplementary Figure 5, Katsuki S et al

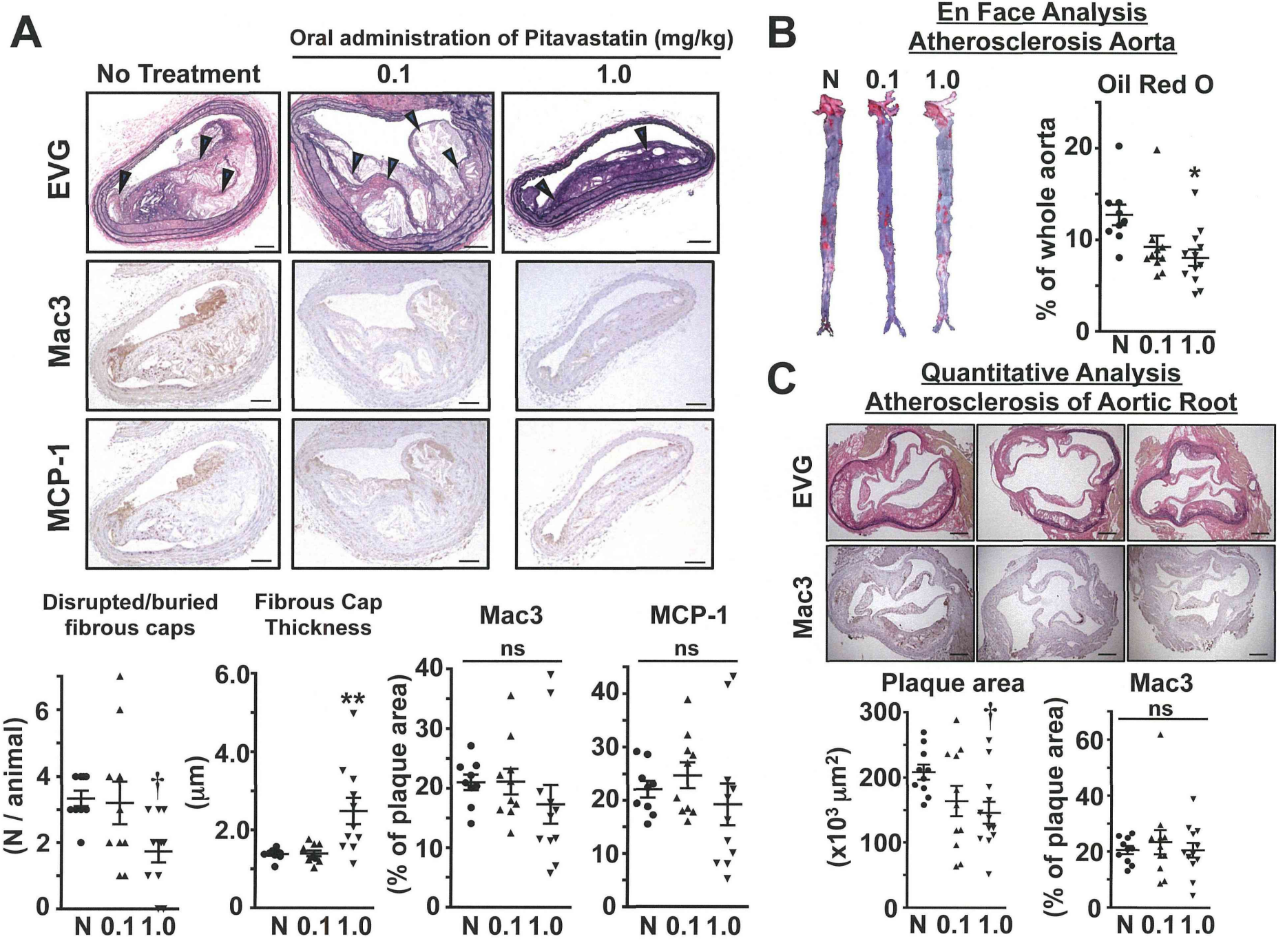

Nanoparticle-Mediated Drug Delivery System for Cardiovascular Disease

Tetsuya MATOBA,[1] MD *and* Kensuke EGASHIRA,[1,2] MD

SUMMARY

Administration of drugs and other therapeutic agents has been the central strategy of contemporary medicine for cardiovascular disease. The use of a drug delivery system (DDS) is always demanded to enhance the efficacy and safety of therapeutic agents, and improve the signal-to-noise ratio of imaging agents. Nano-scale materials modify in vivo drug kinetics, depending on (patho)physiological mechanisms such as vascular permeability and incorporation by the mononuclear phagocyte system, which constitute 'passive-targeting' properties of nano-DDS. By contrast, an 'active-targeting' strategy employs a specific targeting structure on nano-DDS, which binds to the target molecule that is specific for a certain disease process, such as tumor specific antigens and the induction of adhesion molecules. In this review, we summarize recent studies that applied nano-DDS for the diagnosis and treatment of cardiovascular disease, especially focusing on atherosclerosis and myocardial ischemia-reperfusion (IR) injury. Pathophysiological changes in atherosclerosis and myocardial IR injury are successfully targeted by nano-DDS and preclinical studies in animals showed positive effects of nano-DDS enhancing efficacy and reducing adverse effects. The development of nano-DDS in clinical medicine is keenly being awaited. (Int Heart J 2014; 55: 281-286)

Key words: Nanotechnology, Atherosclerosis, Myocardial infarction, Ischemia reperfusion, Inflammation

Nanoparticle-Mediated Drug Delivery Systems

Administration of drugs and other therapeutic agents has been the central strategy of contemporary medicine, based on the concept that a certain disease is caused by a formation of abnormal or diseased cells within healthy organs and the body. In order for drugs to affect disregulated organs and cells, drugs need to overcome physiological barriers, namely circulation to organs, and tissue to cells, and reach target molecules within the cells. On the other hand, all drugs possess potential toxicity that may limit their safe dose and thereby therapeutic efficacy. Targeting drugs to diseased organs/cells may reduce the potential risks of adverse effects; therefore, the use of a drug delivery system (DDS) is always needed to enhance the efficacy and safety of therapeutic agents, and overcome any drawbacks of the agents, such as toxicity, low water solubility, poor bioavailability, and low organ specificity. Moreover, targeting delivery is a desirable property for diagnostic purposes as it improves the signal-to-noise ratio and optimizes sensitivity and specificity.

Recent application of nanotechnology to medicine has developed nanoparticle-mediated DDS (nano-DDS), which modifies the in vivo kinetics of therapeutic and diagnostic agents. One of the most important motives for nano-DDS is drug targeting, which may utilize physiology and pathophysiological properties unique to certain disease processes.[1,2] Nano-DDS can be composed of a variety of materials and structures, including lipids to form micelles or liposomes,[3,4] polymers,[5-7] dendrimers,[8] carbon nanotubes, and metallic nanoparticles such as crystalline iron oxide and gold nanoparticles(Figure 1).[9] Here we describe selected examples of nano-scale materials tested as nano-DDS. Micelles are formed from lipids and other amphiphilic artificial molecules such as polymers.[10] Micelles self-assemble in aqueous solution and may incorporate hydrophobic therapeutic agents to overcome solubility problems. The size (usually 10-100 nm in diameter) and the enclosed space are more confined to those of liposomes (Figure 1A). Liposomes mainly consist of phospholipids that form bilayers with an aqueous phase inside, and are heterogeneous in size, often ranging from a few hundreds to thousands of nanometers in diameter. Liposomes are the most extensively tested nano-DDS in basic and clinical medicine with United States Food and Drug Administration (FDA) approval. Chemicals, nucleotides, and also crystalline metals are incorporated in liposomes (Figure 1B).[3,4] Currently, two polymers, polylactide (PLA) and poly(lactide-co-glycolide) (PLGA), are used for the synthesis of FDA-approved polymeric biodegradable nano-DDS.[2] PLGA polymers may incorporate hydrophilic and hydrophobic therapeutic agents including chemicals and nucleotides by emulsion solvent diffusion methods, and are being tested for intractable diseases including cardiovascular disease (Figure 1C).[11-20] Dendrimers are highly branched macromole-

From the Departments of [1] Cardiovascular Medicine and [2] Cardiovascular Research, Development, and Translational Medicine, Kyushu University Graduate School of Medical Sciences, Fukuoka, Japan.

Address for correspondence: Tetsuya Matoba, MD, Department of Cardiovascular Medicine, Kyushu University Graduate School of Medical Sciences, 3-1-1 Maidashi Higashi-ku, Fukuoka, Fukuoka 812-8582, Japan. E-mail: matoba@cardiol.med.kyushu-u.ac.jp

Received for publication May 9, 2014. Revised and accepted June 2, 2014.

Released in advance online on J-STAGE June 17, 2014.